

**ORIGINAL  
RESEARCH**

R. Kadirvel  
D. Dai  
Y.H. Ding  
M.A. Danielson  
D.A. Lewis  
H.J. Cloft  
D.F. Kallmes

# Endovascular Treatment of Aneurysms: Healing Mechanisms in a Swine Model Are Associated with Increased Expression of Matrix Metalloproteinases, Vascular Cell Adhesion Molecule-1, and Vascular Endothelial Growth Factor, and Decreased Expression of Tissue Inhibitors of Matrix Metalloproteinases

**BACKGROUND AND PURPOSE:** The mechanism of aneurysm healing after coiling remains poorly understood. The purpose of the study was to obtain a better understanding of the cellular and molecular events that are associated with aneurysm healing after endovascular coiling in a swine aneurysm model.

**MATERIALS AND METHODS:** Twenty sidewall aneurysms were created surgically in common carotid arteries in 10 swine. These aneurysms were embolized immediately after creation by using platinum coils by endovascular means. Two and 12 weeks after implantation, aneurysm samples were collected for histologic and biochemical analysis.

**RESULTS:** All aneurysms were completely or nearly completely occluded angiographically at the time of embolization and at follow-up. At 2 weeks, aneurysm cavities were filled with inflammatory cells and myofibroblasts. At 12 weeks, aneurysm cavities were filled with richly vascularized fibrous tissue and disorganized collagen bundles. The expression of matrix metalloproteinase (MMP)-2 and -9 was found to be elevated at 2 weeks. Expression remained greater than that in control tissue at 12 weeks but was significantly decreased compared with the earlier time point. Expression of tissue inhibitors of MMPs (TIMPs) was diminished at both time points. Expression of vascular cell adhesion molecule-1 (VCAM-1) and vascular endothelial growth factor (VEGF) was elevated at both 2 weeks and 12 weeks. Endothelial nitric oxide synthase expression was not different from that in controls. Transforming growth factor-beta expression was elevated at 2 weeks only.

**CONCLUSION:** The coil occlusion in this model that is prone to heal is associated with increased expression of MMP-2, MMP-9, VCAM-1, and VEGF, and decreased expression of TIMPs.

Saccular intracranial aneurysms are characterized pathologically by a chronic inflammatory infiltrate, loss of medial elastin, and thinning of the vessel wall.<sup>1</sup> Endovascular treatment of intracranial aneurysms with detachable coils has been widely used as an important alternative to surgical clipping.<sup>2-4</sup> Even though widely applied, endovascular coils have substantial shortcomings, including high rates of recanalization in large aneurysms.<sup>5,6</sup>

Endovascular interventions address structural consequences of the pathology rather than its biologic basis. Efforts in this field have focused on the development of new devices or on modification of coils in an attempt to change biologic reaction after embolization. To our knowledge, there are few studies focused on the understanding of the biologic responses to embolization and to the healing phenomena. An improved

understanding of the cellular and molecular events related to aneurysm healing might allow rational design of next-generation microcoils.

Synthesis and remodeling of the extracellular matrix components by a variety of cell types is likely one of the major determinants of healing of aneurysms.<sup>7,8</sup> Little is known regarding the relationship between flow, protein expression, and neointima formation and healing, or recurrence after embolization.<sup>9</sup> The healing of aneurysms is associated with the neointima formation, and there may be a conceptual link between recanalization and angiogenesis.<sup>9,10</sup>

The swine model of aneurysms has been widely applied for testing of endovascular occlusion devices.<sup>11,12</sup> This model has demonstrated that a thick layer of neointima forms along the aneurysm neck following embolization with platinum coils.<sup>11</sup> The purpose of this study was to characterize the vascular remodeling in swine aneurysms after embolization with platinum coils. We have studied cells involved in the healing of aneurysms as well as the expression of proteins involved in matrix remodeling and cell migration (matrix metalloproteinases [MMPs]-2 and -9) and their inhibitors (tissue inhibitors of MMPs [TIMPs]-1 and -2), angiogenesis growth factors (vascular endothelial growth factor [VEGF] and transforming

Received April 13, 2006; accepted after revision September 6.

From the Neuroradiology Research Laboratory, Department of Radiology, Mayo Clinic College of Medicine, Rochester, Minn.

This work was supported by a research grant from National Institutes of Health (NS42646-01).

Paper previously presented at: Annual Meeting of the American Society of Neuroradiology, May 21-27, 2005; Toronto, ON, Canada.

Please address correspondence to David F. Kallmes, MD, Mayo Clinic College of Medicine, 200 First St SW, Rochester, MN 55905; e-mail: Kallmes.david@mayo.edu

growth factor-beta [TGF- $\beta$ ]), and adhesion molecule (vascular cell adhesion molecule-1 [VCAM-1]).

## Materials and Methods

### Sidewall Aneurysm Model

All animal experiments were conducted in accordance with policies set by the Institutional Animal Care and Use Committee at our institution. Sidewall aneurysms were created in 10 female domestic swine (body weight, 30–40 kg) by using the methods of German and Black.<sup>13</sup> Briefly, anesthesia was achieved by using tiletamine (Telazol, 5 mg/kg) and xylazine (1.0 mg/kg) administered intramuscularly and was maintained by using inhaled isoflurane gas 1%–3%. Using sterile technique, the surgeon made a midline neck incision. The right external jugular vein was exposed and isolated, and two 4-cm lengths of vein were harvested and placed in sterile saline. The right carotid artery was exposed, cleaned of adventitia, and clamped with DeBakey vascular clamps proximally and distally. After achieving stasis in this isolated segment, the surgeon made an arteriotomy approximately 7 mm in diameter and performed an end-to-side anastomosis (vein to artery) by using 7–0 Prolene interrupted sutures. When the surgeon was satisfied with the anastomosis, the proximal clamp was released, and blood flow was re-established through the artery and aneurysm. A similar technique was used in creating an aneurysm along the left common carotid artery. The resulting aneurysms were then immediately embolized with platinum coils.

### Embolization Procedure

Because the swine model has a strong tendency for spontaneous thrombosis<sup>12</sup> once the aneurysm is created, it was immediately embolized. A cut-down was performed to gain access to the right common femoral artery (FA). A 6F sheath was placed and connected to continuous heparinized saline flush. Systemic anticoagulation was achieved with intravenous heparin (150-U/kg bolus). A 6F guiding catheter was placed over an angled guidewire into the proximal right common carotid artery. A microcatheter was then inserted coaxially through the guiding catheter into the aneurysm cavity. Digital subtraction angiography (DSA) was performed with injection of 5 mL of iodinated contrast medium (Omnipaque 300, Nycomed, Princeton, NJ). Aneurysms were as densely packed as possible with platinum coils. In all cases, balloon assistance was used to protect the coils from herniating into the parent vessel and to facilitate coil placement.

### Harvest Procedures

Vessels in 5 subjects (10 aneurysms) were harvested at 2 weeks following embolization and in 5 subjects (10 aneurysms) were harvested at 12 weeks following embolization. With the subject under general anesthesia, the left common FA was accessed by using a percutaneous technique. A 5F sheath was placed. A 5F diagnostic catheter was placed sequentially into each embolized vessel, and DSA was performed. The angiographic occlusion scores were calculated on the basis of percentage of contrast of iodinated contrast medium inside the aneurysm cavity. Following DSA, the animals were euthanized. Immediately before sacrifice, 10 mL of heparin (1000 U/mL) was injected into each animal to prevent blood clotting. Then the embolized vessels were harvested. The samples were either frozen in liquid nitrogen or placed in buffered formalin. The gross appearance of the neck of the aneurysm was carefully examined and photographed. For each subject, 1 aneurysm was used for histologic examination and the contralateral aneurysm was used for molecular biologic studies.

### Histopathology

After fixing the tissue in 10% buffered formalin for at least 24 hours, we dehydrated the tissues in an ascending series of ethanol, cleared them in xylene, embedded them in paraffin, and sectioned them at 1000- $\mu$ m intervals in a coronal orientation. Coil fragments were carefully removed. Sections were re-embedded in paraffin and sectioned at 5- $\mu$ m intervals. Sections were stained with hematoxylin-eosin (H&E) for conventional histopathologic evaluation. The Vectastain Elite ABC system (Vector Laboratories, Burlingame, Calif) was used for immunohistochemical staining of smooth muscle actin (SMA) and vimentin as described previously.<sup>11</sup>

### Molecular Biology

The parent artery (PA) at the level of the aneurysm, the proximal parent artery (PPA), and the distal parent artery (DPA) were dissected. Aneurysm samples were dissected into 2 sections, including the neck and dome. Coils from both neck and dome were removed carefully. Extreme care was taken to minimize loss of cells. A segment of the jugular vein (JV) was used as a control for aneurysm tissue, whereas a segment of FA was used as a control for PA tissue. Samples were kept frozen at  $-70^{\circ}\text{C}$  until use.

### Sample Preparation

Frozen samples were pulverized under liquid nitrogen and extracted in ice cold lysis buffer (10-mmol/L sodium phosphate, pH 7.2, 150-mmol/L sodium chloride [NaCl], 1% Triton X-100 [Union Carbide, Bound Brook, NJ], 0.1% sodium dodecyl sulfate [SDS], 0.5% sodium deoxycholate, and 0.2% sodium azide). After centrifugation at 10,000 g for 20 minutes at  $4^{\circ}\text{C}$ , the protein concentration of the supernatant was determined.

### Gelatin Zymography

Protein samples (20- $\mu$ g protein per lane) were resolved by nonreducing 10% SDS-polyacrylamide gel electrophoresis (PAGE) through gels containing 0.1% gelatin. Gels were washed with 2.5% Triton X-100 for 1 hour, then incubated for 24 hours at  $37^{\circ}\text{C}$  in developing buffer (50-mmol/L Tris-hydrochloric acid [HCl]), pH 8.5, 5-mmol/L calcium chloride, and 0.5-mmol/L zinc chloride). Gelatinolytic zones were visualized after staining the gels with 0.5% Coomassie Blue R-250 (Pierce Biotechnology, Rockford, Ill). Densitometric analyses of gelatinolytic zones were analyzed with the use of UN-SCAN-IT software (Silk Scientific, Orem, Utah).

### Western Blotting

Protein samples (50- $\mu$ g protein per lane) were resolved by SDS-PAGE under reduced conditions, transferred to polyvinylidene fluoride membrane, blocked with 5% nonfat dry milk in Tris-buffered saline solution with Tween (TBST) (20-mmol/L Tris-HCl, pH 7.5, 0.15-mol/L NaCl and 0.01% Tween 20), then incubated overnight at  $4^{\circ}\text{C}$  with appropriately diluted mouse anti-human MMP-2 (Chemicon, Temecula, Calif), MMP-9 (Chemicon), TIMP-1 (Oncogene, Carpinteria, Calif), TIMP-2 (Oncogene), endothelial nitric oxide synthase (eNOS) (BD Biosciences, Mississauga, ON, Canada), VCAM-1 (Santa Cruz Biotech, Santa Cruz, Calif), VEGF, TGF- $\beta$  (Chemicon), and  $\beta$ -actin (Sigma-Aldrich Canada, Oakville, ON, Canada). The antibodies against human proteins are known to cross-react with porcine proteins. Peroxidase conjugated goat anti-mouse immunoglobulin G (Oncogene) was used as the secondary antibody, and immune complexes were visualized by the enhanced chemiluminescence method. The intensities of protein bands were determined by using UN-

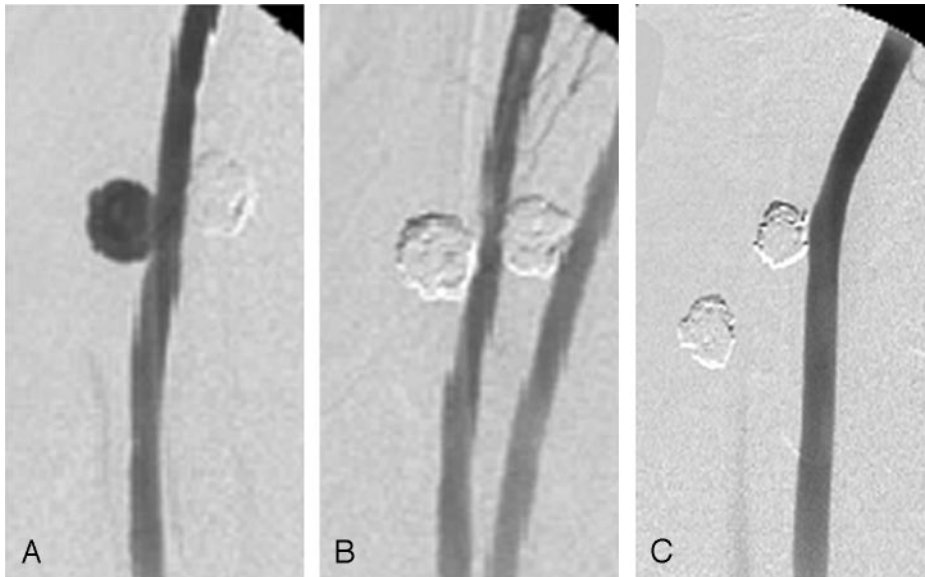


**Fig 1.** A, Angiogram of experimental aneurysm created on the common carotid artery of swine pre-embolization shows contrast filling of the aneurysm dome. B, Postembolization angiogram of aneurysm with platinum coils. Aneurysm is tightly packed with platinum coils. C, Angiogram of 12-week follow-up shows complete occlusion of aneurysm from the parent artery, suggesting the formation of a neointimal layer.

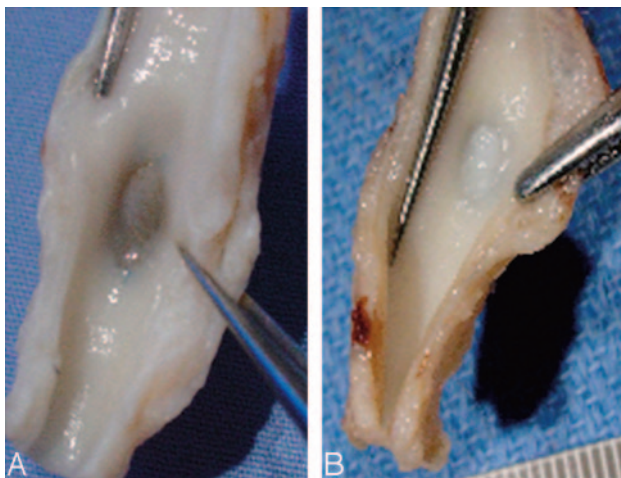


**Fig 2.** Gross photographs showing a thin to moderately thick membranous tissue at the neck of a 2-week aneurysm (A) and a thick membranous tissue at the neck of a 12-week aneurysm (B).

SCAN-IT software. Results are expressed in arbitrary units and adjusted for  $\beta$ -actin levels.

### Statistical Analyses

Results are expressed as mean  $\pm$  SD. Each group consisted of 5 animals. Differences between groups were assessed by analysis of variance followed by the Tukey contrast test. Statistical significance was taken as a  $P$  value of  $< .05$ . The JV was used as the control for aneurysm tissues, whereas the FA was used as the control for PA tissues.

## Results

### Angiographic Findings

All aneurysms were embolized without any technical complications and without acute or chronic morbidity or mortality. Balloon-assisted embolization was performed for all aneurysms. In both the 2- and 12-week groups, all aneurysms were as tightly packed as possible with platinum coils. Representative angiograms are shown in Fig 1. On the basis of the DSA

studies, the mean aneurysm neck diameter, width, and height were 5.38 mm, 10.31 mm, and 8.56 mm, respectively, at 2 weeks and 5.84 mm, 9.75 mm, and 8.24 mm at 12 weeks. The difference in aneurysm dimensions at these 2 time points was not statistically significant.

Angiographic occlusion scores (complete occlusion/near-complete occlusion/incomplete occlusion) immediately following embolization were 9/1/0 and 5/5/0 for 2-week and 12-week groups, respectively. At follow-up, the scores were 8/2/0 and 10/0/0 at 2 weeks and 12 weeks, respectively.

Macroscopic findings showed thin to moderately thick fibrous neointimal membranes covering the aneurysms harvested at 2 weeks and very thick fibrous neointimal membranes covering the aneurysms harvested at 12 weeks (Fig 2).

### Pathologic Findings

At 2 weeks, 3 of 5 aneurysm lumens were filled with attenuated inflammatory tissue and residual scattered poorly organized thrombus (Fig 3A). The remaining 2 aneurysms harvested at 2 weeks were filled with attenuated tissue primarily consisting of elongated spindle cells and inflammatory cells (Fig 3B). These spindle cells were positive for SMA and vimentin (Fig 3C), indicating myofibroblastic differentiation. Well-developed neointimal membranes consisting of large numbers of myofibroblasts were seen across the necks at 2 weeks.

Three of 5 aneurysms harvested at 12 weeks showed highly vascularized fibrous tissue filling the aneurysm domes, with abundant attenuated disorganized collagen bundles (Figs 3D). The cellular bundles within the fibrous matrix were positive for SMA and vimentin, indicating myofibroblastic differentiation. Two of 5 aneurysms harvested at 12 weeks demonstrated attenuated chronic inflammatory tissue, primarily consisting of lymphocytes, histocytes, and giant cells, along with thin-walled vessels within the dome (Fig 3E). Thick neointimal membranes, on the order of 1000- $\mu$ m thickness, were seen across the necks at 12 weeks.

### Biochemical Findings

Gelatin zymography of MMP-2 and MMP-9 at 2 and 12 weeks after embolization of the aneurysms is shown in Fig 4. At both 2 weeks and 12 weeks, compared with control venous tissue, a significant increase in pro- and active-MMP-2 and pro- and active-MMP-9 was seen in the neck and dome. Expression of active collagenases was significantly elevated within the adjacent PA compared with the control FA and JV ( $P < .05$ ). The

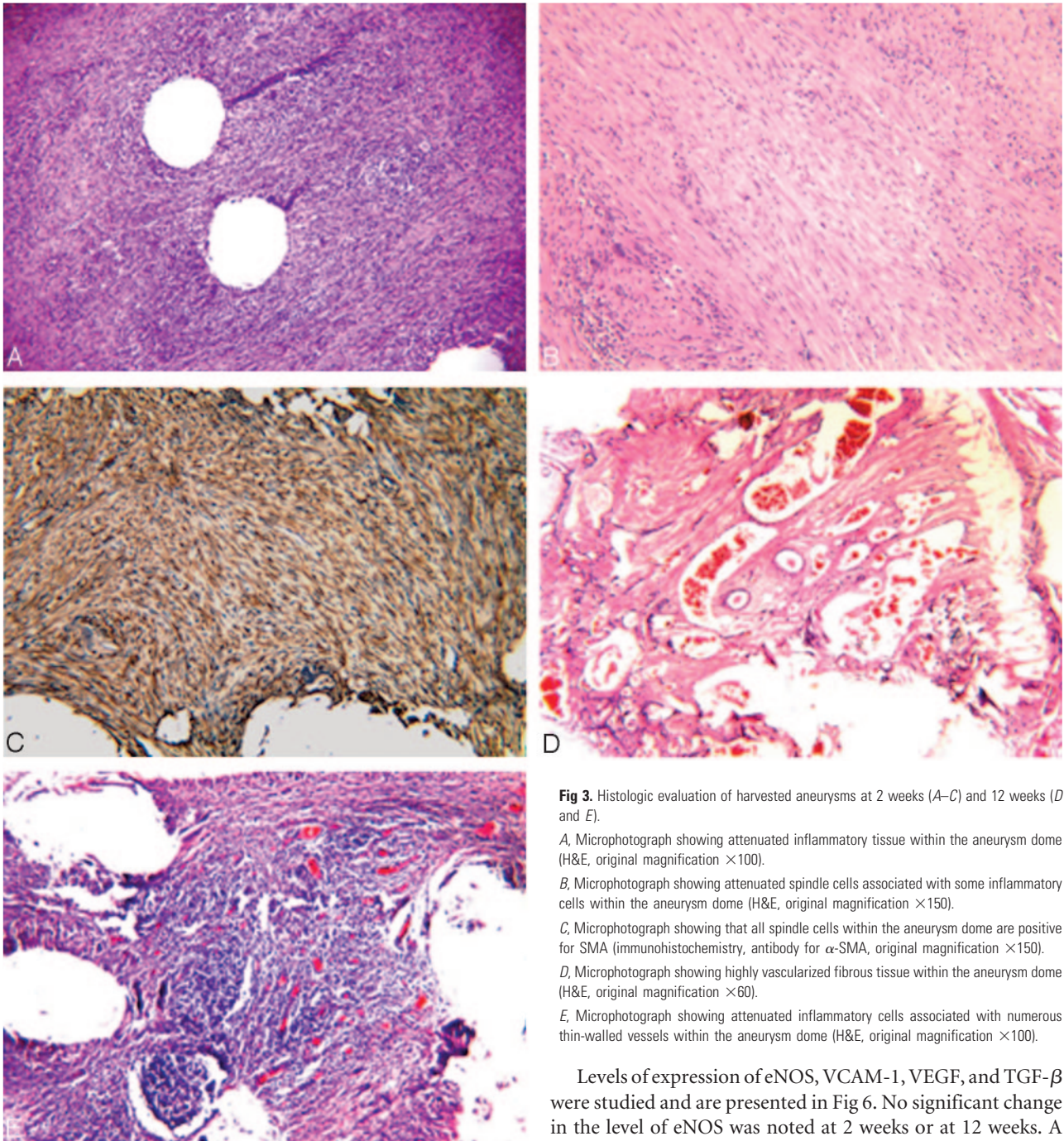


**Fig 3.** Histologic evaluation of harvested aneurysms at 2 weeks (A–C) and 12 weeks (D and E).

A, Microphotograph showing attenuated inflammatory tissue within the aneurysm dome (H&E, original magnification  $\times 100$ ).

B, Microphotograph showing attenuated spindle cells associated with some inflammatory cells within the aneurysm dome (H&E, original magnification  $\times 150$ ).

C, Microphotograph showing that all spindle cells within the aneurysm dome are positive for SMA (immunohistochemistry, antibody for  $\alpha$ -SMA, original magnification  $\times 150$ ).

D, Microphotograph showing highly vascularized fibrous tissue within the aneurysm dome (H&E, original magnification  $\times 60$ ).

E, Microphotograph showing attenuated inflammatory cells associated with numerous thin-walled vessels within the aneurysm dome (H&E, original magnification  $\times 100$ ).

activities of these collagenases decreased at 12 weeks compared with the corresponding 2-week aneurysm segments ( $P < .001$  for both MMP-2 and MMP-9 compared with 2-week data). Compared with that of controls, expression of these collagenases remained slightly elevated at 12 weeks. However, at both 2 weeks and 12 weeks, there were no significant differences in the levels of MMP-2 and MMP-9 in the proximal and distal PAs compared with control arteries. These results were also confirmed by Western blot analysis (data not shown).

Expression of TIMP-1 and TIMP-2 and their densitometric measurements are shown in Fig 5. The aneurysm neck and dome showed a highly significant decrease in the levels of both TIMP-1 and TIMP-2 at 2 weeks ( $P < .001$ ) and 12 weeks compared with those in the control vessels ( $P < .05$ ).

Levels of expression of eNOS, VCAM-1, VEGF, and TGF- $\beta$  were studied and are presented in Fig 6. No significant change in the level of eNOS was noted at 2 weeks or at 12 weeks. A significant elevation in the expression of VCAM-1 and VEGF was observed in the neck and dome at 2 weeks and at 12 weeks. TGF- $\beta$  expression was found to be high at 2 weeks only; its expression was not different from that of the controls 12 weeks after embolization.

### Discussion

Even though platinum coils have been applied clinically for more than a decade, precise understanding of the mechanisms involved in aneurysm healing or recurrence following embolization remains poor. In this study, we used experimental aneurysms in swine to study the expression of important vascular proteins following embolization. We acknowledge that the swine model has substantial limitations as a model of intracranial aneurysms, including a propensity to undergo

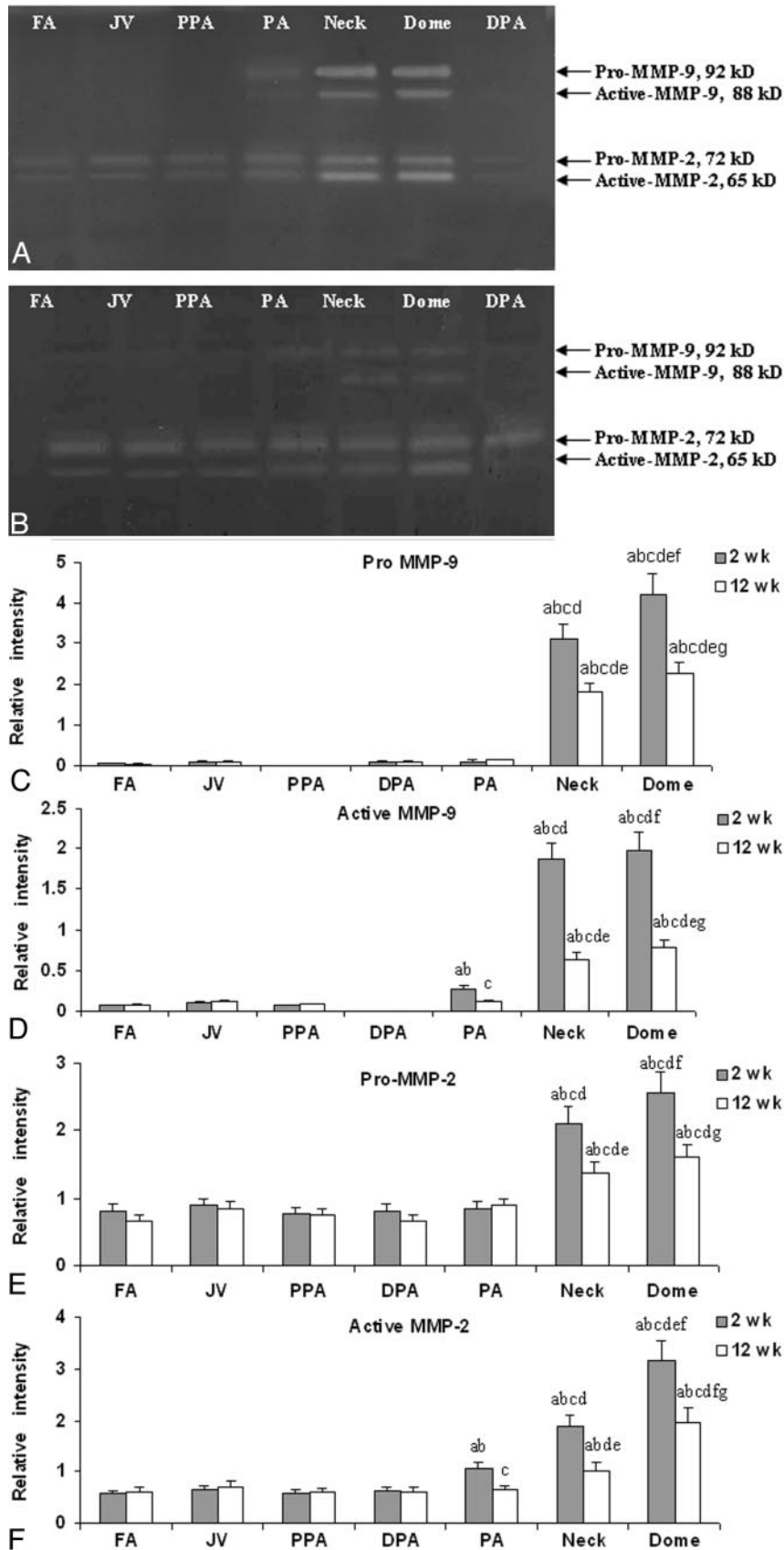


**Fig 4.** A representative gelatin zymogram of MMP-2 and MMP-9 from pigs at 2 weeks (A) and 12 weeks (B) after embolization. Densitometric analysis of gelatin zymogram of pro-MMP-9 (C), active-MMP-9 (D), pro-MMP-2 (E), and active-MMP-2 (F) at both 2-week and 12-week time points. Labels a–g represent  $P < .05$  compared with FA, JV, PPA, and DPA at 2 weeks (a); FA, JV, PPA, and DPA at 12 weeks (b); PA at 2 weeks (c); PA at 12 weeks (d); the neck at 2 weeks (e); the neck at 12 weeks (f); and the dome at 2 weeks (g).

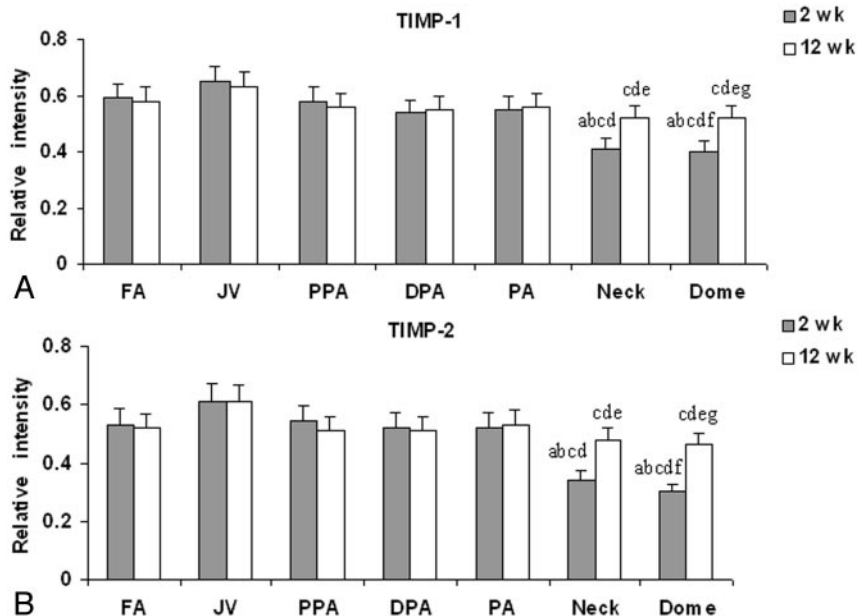


**Fig 5.** Densitometric analysis of Western blot of TIMP-1 (A) and TIMP-2 (B) expressions at 2-week and 12-week time points. Labels a and b represent  $P < .05$ ; labels a–g represent  $P < .05$  compared with FA, PPA, PA and DPA at 2 weeks (a); FA, PPA, PA, and DPA at 12 weeks (b); JV at 2 weeks (c); JV at 12 weeks (d); the neck at 2 weeks (e); the neck at 12 weeks (f); and the dome at 2 weeks (g).

spontaneous thrombosis as well as robust healing even with standard platinum coils. However, the model still offers a technique for the study of the molecular biologic processes in well-healed aneurysms and may guide researchers focused on improved healing of saccular aneurysms after coiling.

In this study, we focused on proteins highly associated with vascular healing or recurrence, as well as markers of endothelial cell function and angiogenesis. Recurrences may be delayed months or years, yet we have focused on early changes. However, Raymond et al<sup>6</sup> showed that almost half of all recurrences were present by 6 months after coiling. Furthermore, because most practitioners obtain follow-up angiograms at 6 months, without earlier angiograms before that point, reports in the literature are not available, to the best of our knowledge, indicating whether the recurrences diagnosed at 6 months occurred within days, weeks, or months. Thus, early changes may be of substantial importance.

We noted marked elevation of both MMP-2 and -9 early after embolization. After 12 weeks, expression of the MMPs had diminished compared with that in the earlier time point but was still greater than that of controls. Expression of MMP inhibitors was low at both time points. These findings suggest that active vascular response is present early after embolization.

MMPs are calcium- and zinc-dependent endopeptidases. MMPs have a central role in the degradation of extracellular components and are important for thrombus organization.<sup>14,15</sup> MMPs also participate in the proliferation and migration of smooth-muscle cells to develop neointima during wound healing.<sup>16,17</sup> MMPs are produced by various cell types including inflammatory cells. Increased expression of MMPs after embolization is attributed to the presence of inflammatory cells at the neck and dome of the aneurysm. MMP activities are regulated by their tissue inhibitors, TIMPs, which are used to control neointima formation.<sup>18,19</sup> The increased activ-

ities of MMP-2 and -9 and decreased levels of TIMP-1 and -2 at both 2 weeks and 12 weeks after embolization correlate with the neointima formation at the aneurysm neck. Relative decreases in MMPs at 12 weeks compared with 2 weeks suggest that important cellular functions may occur early after treatment. This finding suggests that alterations in coil technology aimed at diminished recanalization<sup>20,21</sup> should occur early after coil implantation rather than in delayed fashion. The increased activities of MMPs in the PA may be due to surgical trauma associated with the aneurysm creation and embolization procedures.

There are a number of factors associated with tissue remodeling whose expression is related to extracellular matrix turnover. VEGF is essential for endothelial cell differentiation (vasculogenesis) and plays a major role in neovascularization in a variety of disease states. VEGF elicits an array of biologic responses in vascular cells, including cell proliferation and migration, increased vascular permeability, and the production of the potent vasodilators nitric oxide and prostacycline. Increased expression of VEGF correlates with the endothelial cell differentiation and subsequent neointima formation during the postembolization period.

The interactions between leukocytes and the endothelial cell membrane are a key factor in all inflammatory-mediated remodeling processes. The normal arterial endothelium expresses VCAM at very low levels. VCAM-1 holds particular interest because it binds leukocytes (monocytes and lymphocytes) that accumulate in injured lesions and it can stimulate angiogenesis.<sup>22</sup> The enhanced expression of VCAM in platinum coil-embolized aneurysms is associated with the adhesion of inflammatory cells associated with the aneurysm wall. Elevated levels of VCAM may explain the increase of neovascularity in the coiled aneurysms. Increased expression of VCAM-1 and VEGF, despite the lack of recanalization in this model, suggests that these proteins may be related to neovas-

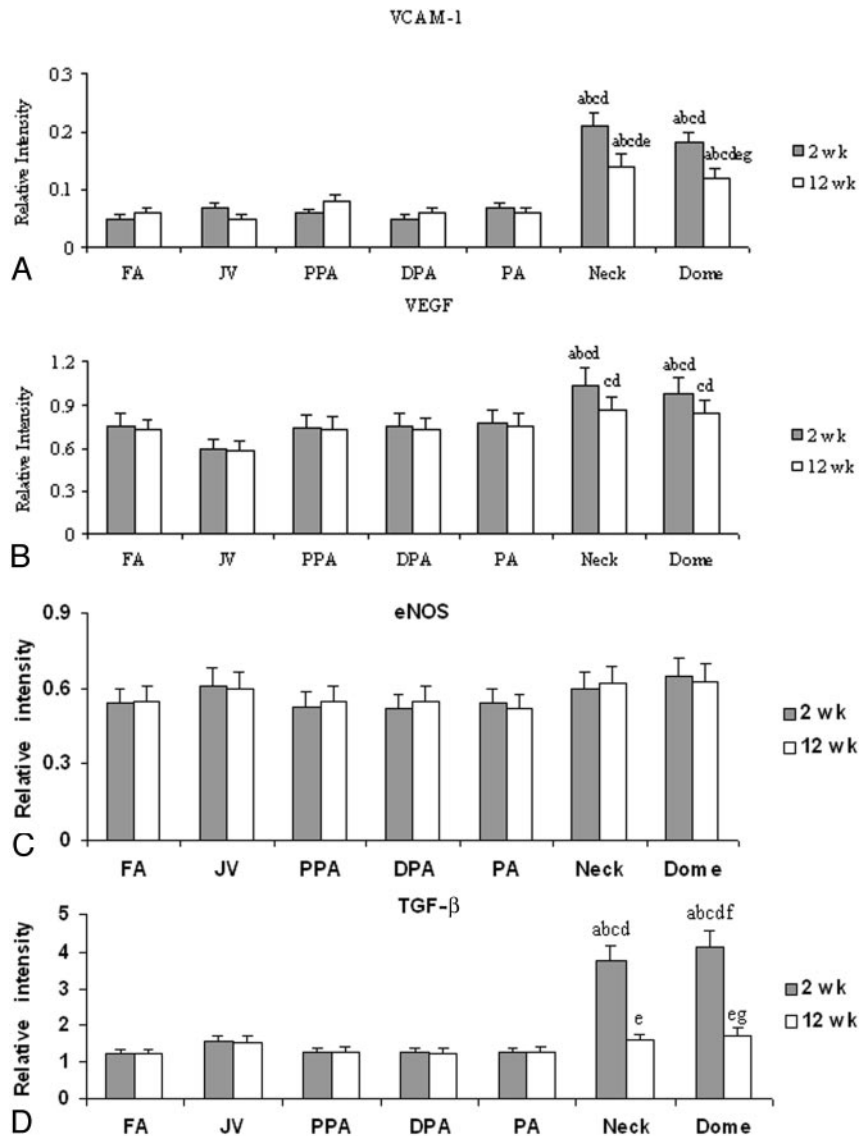


**Fig 6.** Densitometric analysis of Western blot of VCAM-1 (A), VEGF (B), eNOS (C), and TGF- $\beta$  (D) expressions at 2-week and 12-week time points. Labels a and b represent  $P < .05$ ; labels a–g represent  $P < .05$  compared with FA, PPA, PA, and DPA at 2 weeks (a); FA, PPA, PA, and DPA at 12 weeks (b); JV at 2 weeks (c); JV at 12 weeks (d); the neck at 2 weeks (e); the neck at 12 weeks (f); and the dome at 2 weeks (g).

cularization of the organizing clot,<sup>23</sup> and the expression of these proteins is not associated with angiogenesis as evidenced by histopathology. However, further experiments will be needed to show an association between the expression of VCAM, VEGF, and recanalization after coiling.

The TGF isoforms have profibrotic functions and promote healing. TGF expression is increased in normal wound healing, and exogenous administration of this growth factor to wounds increases collagen, proteoglycans, and inflammatory cell accumulation.<sup>24</sup> TGF- $\beta$  has been shown to induce vascular smooth-muscle cell migration and synthesis of extracellular matrix and inhibits proteolysis and endothelial cell migration. The initial increased TGF- $\beta$  expression may be interpreted as a sign of TGF-mediated healing. TGF- $\beta$  may not be involved in chronic healing, as evidence by its lowered expression chronically. These findings are in accordance with study of Ribourtout et al,<sup>25</sup> in which a gene therapy study of TGF- $\beta$  overexpression for endovascular treatment did not heal aneurysms significantly.

We acknowledge that the study is purely observational and that biochemical findings cannot be proved causal or necessary. However, more robust experimentation would likely require experiments such as microarrays of protein and gene expression or those using knockout mice and is thus not easily undertaken. Moreover, there are relative weaknesses in this study, including the fact that balloon assistance was needed in these cases to avoid parent artery compromise and loss of a few cells when removing coils from the aneurysm. Finally, as noted in the “Discussion” and previously, early embolization is mandatory in swine studies because of the propensity toward spontaneous thrombosis.

### Conclusion

We aimed to study the expression of some important cellular as well as extracellular molecules involved in the vascular remodeling of aneurysms embolized with platinum coils. The coil occlusion in this model that is prone to heal is associated with increased expression of MMP-2, MMP-9, VCAM-1, and

VEGF and decreased expression of TIMPs. A detailed study probing the molecular pathways that lead to aneurysm healing will be important for better understanding of the healing mechanism.

### Acknowledgment

We thank Dr. Zvonimir Katusic, Department of Anesthesiology, for his generous help on the project.

### References

1. Ruigrok YM, Rinkel GJ, Wijmenga C. Genetics of intracranial aneurysms. *Lancet Neurol* 2005;4:179–89
2. Molyneux AJ, Kerr RS, Yu LM, et al. International subarachnoid aneurysm trial (ISAT) of neurosurgical clipping versus endovascular coiling in 2143 patients with ruptured intracranial aneurysms: a randomised comparison of effects on survival, dependency, seizures, rebleeding, subgroups, and aneurysm occlusion. *Lancet* 2005;366:809–17
3. Bavinszki G, Talazoglu V, Killer M, et al. Gross and microscopic histopathological findings in aneurysms of the human brain treated with Guglielmi detachable coils. *J Neurosurg* 1999;91:284–93
4. Guglielmi GVF, Sepetka I, Macellari V. Electrothrombosis of saccular aneurysms via endovascular approach. Part 1. Electrochemical basis, technique, and experimental results. *J Neurosurg* 1991;75:1–7
5. Hayakawa M, Murayama Y, Duckwiler GR, et al. Natural history of the neck remnant of a cerebral aneurysm treated with the Guglielmi detachable coil system. *J Neurosurg* 2000;93:561–68
6. Raymond J, Guilbert F, Weill A, et al. Long-term angiographic recurrences after selective endovascular treatment of aneurysms with detachable coils. *Stroke* 2003;34:1398–403
7. Peters DG KA, Feingold E, Heidrich-O'Hare E, et al. Molecular anatomy of an intracranial aneurysm: coordinated expression of genes involved in wound healing and tissue remodeling. *Stroke* 2001;32:1036–42
8. Fujiwara NH, Kallmes DF. Healing response in elastase-induced rabbit aneurysms after embolization with a new platinum coil system. *AJNR Am J Neuroradiol* 2002;23:1137–44
9. Raymond J, Ogoudikpe C, Salazkin I, et al. Endovascular treatment of aneurysms: gene expression of neointimal cells recruited on the embolic agent and evolution with recurrence in an experimental model. *J Vasc Interv Radiol* 2005;16:1355–63
10. Ribourtout E, Raymond J. Gene therapy and endovascular treatment of intracranial aneurysms. *Stroke* 2004;35:786–93
11. Dai D, Ding YH, Danielson MA, et al. Histopathologic and immunohistochemical comparison of human, rabbit, and swine aneurysms embolized with platinum coils. *AJNR Am J Neuroradiol* 2005;26:2560–68
12. Murayama YVF, Suzuki Y, Akiba Y, et al. Development of the biologically active Guglielmi detachable coil for the treatment of cerebral aneurysms. Part II: An experimental study in a swine aneurysm model. *AJNR Am J Neuroradiol* 1999;20:1992–99
13. German W, Black S. Experimental production of carotid aneurysms. *N Engl J Med* 1954;3:463–68
14. Fontaine VJM, Houard X, Rossignol P, et al. Involvement of the mural thrombus as a site of protease release and activation in human aortic aneurysms. *Am J Pathol* 2002;161:1701–10
15. Kuzuya MIA. Role of matrix metalloproteinases in vascular remodeling. *J Athroscler Thromb* 2003;10:275–82
16. Cho M, Reidy MA. Matrix metalloproteinase-9 is necessary for the regulation of smooth muscle cell replication and migration after arterial injury. *Circ Res* 2002;91:845–51
17. George SJ, Zaltsman AB, Newby AC. Surgical preparative injury and neointima formation increase MMP-9 expression and MMP-2 activation in human saphenous vein. *Cardiovasc Res* 1997;33:447–59
18. Furman CLZ, Walsh K, Duverger N, et al. Systemic tissue inhibitor of metalloproteinase-1 gene delivery reduces neointimal hyperplasia in balloon-injured rat carotid artery. *FEBS Lett* 2002;531:122–26
19. George SJ BA, Angelini GD, Newby AC. Gene transfer of tissue inhibitor of metalloproteinase-2 inhibits metalloproteinase activity and neointima formation in human saphenous veins. *Gene Ther* 1998;5:1552–60
20. Murayama Y, Tatehima S, Gonzalez NR, et al. Matrix and bioabsorbable polymeric coils accelerate healing of intracranial aneurysms: long-term experimental study. *Stroke* 2003;34:2031–37
21. Ding YH, Dai D, Lewis DA, et al. Angiographic and histologic analysis of experimental aneurysms embolized with platinum coils, Matrix, and Hydro-Coil. *AJNR Am J Neuroradiol* 2005;26:1757–63
22. Koch AE, Halloran MM, Haskell CJ, et al. Angiogenesis mediated by soluble forms of E-selectin and vascular cell adhesion molecule-1. *Nature* 1995;376:517–19
23. Chu AJ. Tissue factor mediates inflammation. *Arch Biochem Biophys* 2005;440:123–32
24. Ravanti LHL, Hakkinen L, Larjava H, et al. Transforming growth factor-beta induces collagenase-3 expression by human gingival fibroblasts via p38 mitogen-activated protein kinase. *J Biol Chem* 1999;274:37292–300
25. Ribourtout E, Desfaits AC, Salazkin I, et al. Ex vivo gene therapy with adenovirus-mediated transforming growth factor beta 1 expression for endovascular treatment of aneurysm: results in a canine bilateral aneurysm model. *J Vasc Surg* 2003;38:576–83